Optimized Carbonization and Kinetic Analysis of Palm Kernel Shell Porous Carbon for Heavy Metal Adsorption

Mas Ayu Elita Hafizah[1*], Azwar Manaf[2], Tiara Valency[2], Andreas Andreas[3], and Maykel Manawan[1]

[1]*Department of Weaponry Technology, Faculty of Defense Science and Technology, Universitas Pertahanan Republik Indonesia (UNHAN), Complex of Indonesia Peace and Security Center (IPSC), Sentul, Bogor 16810, Indonesia*

[2]*Department of Physics, Faculty of Mathematics and Natural Sciences, Universitas Indonesia, Depok 16424, Indonesia*

[3]*Research Center of Advanced Chemistry, National Research and Innovation Agency, Puspiptek Area Building 452, Puspiptek, Serpong, Banten 15314, Indonesia*

Corresponding author:

tel: +62-816809488
email: ayu.hafizah@idu.ac.id

Received: October 15, 2024
Accepted: January 6, 2025

DOI: 10.22146/ijc.100714

Abstract: *This study explores the use of porous carbon derived from palm kernel shells to adsorb lead ions (Pb^{2+}) from water. Porous carbon was produced by carbonizing palm kernel shells at different temperatures (400, 600, and 800 °C) and was evaluated for its effectiveness in a lead chloride ($PbCl_2$) solution. The best adsorption rate, reducing Pb^{2+} concentration by 27.5%, was observed by carbonized material at 800 °C with a 3 h contact time. Kinetic analysis suggested that the process followed a pseudo-second-order model, indicating that chemical adsorption was the dominant mechanism. The adsorption data were best described by the Freundlich isotherm, implying multilayer adsorption on an uneven surface. These findings highlight the efficient and low-cost potential of palm kernel shell-based porous carbon for removing heavy metals from wastewater. Palm kernel shell-derived porous carbon has proven to be a sustainable, cost-effective, and practical solution for mitigating Pb^{2+} contamination, positioning it as a promising candidate for environmentally friendly water treatment applications.*

Keywords: *porous carbons; metal absorption; heavy metal; adsorption capacity*

■ INTRODUCTION

Each year, the demand for palm oil increases globally, resulting in a significant increase in oil palm plantations. Indonesia and Malaysia are the two largest palm oil producers in the world, with Indonesia being the top exporter. Indonesia's economy is largely dependent on the palm oil industry, which contributes to economic growth by generating substantial foreign exchange, creating jobs, and contributing to economic growth [1]. By 2015, Indonesia had allocated 10 million hectares of land to oil palm plantations [2]. Each ton of fresh fruit bunches processed, the palm oil industry yields about 20–23% primary palm oil and 5–7% kernel oil product, leaving significant quantities of solid waste. This includes 20–23% empty fruit bunches composed of 70% water and 30% dry matter, along with 10–12% palm fruit fibers and 7–9% palm kernel shells [3].

The composition of palm shells in lignocellulosic biomass is made up of a mix of carbohydrate polymers, with around 40% cellulose, 24% hemicellulose, 21% lignin, and 15% ash. In the palm oil industry, palm shells are typically around 6–7% of the total fresh fruit bunch processed [4]. Palm kernel shells are particularly notable for their high carbon content, about 49.79%. The composition of air-dried palm kernel shells includes hydrogen (H) at 5.58%, oxygen (O) at 34.66%, nitrogen (N) at 0.72%, sulfur (S) at 0.08%, and chlorine (Cl) at 89 ppm [5].

Palm kernel shells offer several benefits, including their potential conversion into porous carbon for industrial applications. The high carbon content makes palm kernel shells a valuable resource, especially for conversion into porous carbon. Processing this porous carbon into briquettes can be done in industrial boilers

or as an alternative energy source, which can contribute to waste reduction and renewable energy production. Additionally, palm kernel shells have shown potential in replacing coarse aggregates in asphalt, Resdiansyah et al. [6] suggesting they can substitute up to 10% of aggregates for high-traffic roads and up to 50% for lighter traffic. When combined with sawdust, they also enhance the fuel's energy content [7]. Palm kernel shells have been evaluated as a substitute for friction linings in brake systems, with performance comparable to asbestos-based materials under static and dynamic conditions [8].

The use of porous carbon in environmental cleanup, air filtration, and various industrial applications is greatly influenced by its high adsorption capacity. The effectiveness of these applications depends on the optimization of the porous carbon's adsorption capacity, which is still a challenge. Although traditional approaches, such as adjusting heating rates or particle sizes, have been explored, they often produce inconsistent results, leaving room for further performance improvements [9].

Porous carbon is well-known for its large surface area, which can be as much as 300 to 2000 m^2/g, and its highly porous structure. These features make it particularly effective at adsorbing gases, vapors, and liquids [10]. The material's pores are categorized into micropores (ranging from 10 to 1000 Å) and macropores (larger than 1000 Å). This structural versatility allows porous carbon to be used across a wide range of applications, including gas purification, catalytic processes, and odor and color removal in the food and medical sectors. Its use as a water filtration medium and for the removal of heavy metal pollutants further underscores its broad utility [11].

In many industries, environmental pollution is frequently caused by the release of liquid waste containing pollutants that exceed regulatory limits. Heavy metals such as lead (Pb), mercury (Hg), and cadmium (Cd) can lead to significant health risks if they are present in industrial waste. These metals can cause various diseases in living organisms, especially in humans, where exposure to contaminated food and water can lead to digestive disorders, kidney damage, cancer, and other toxic effects [12]. Heavy metals are persistent pollutants that do not easily degrade and can accumulate in human tissues, potentially resulting in long-term health issues [13]. Recent studies have explored ways to improve adsorption, but the effects of heating rate and particle size on efficiency remain unclear. In order to optimize conditions for better performance, this study examines how these factors affect porous carbon's adsorption power. The findings will offer insights into improving porous carbon treatment, with the potential for greater efficiency and cost-effectiveness in industrial applications, advancing the field of adsorption technology.

■ EXPERIMENTAL SECTION

Materials

The primary raw material used to produce porous carbon in this study was palm shell samples. These shells, which are known for their abundance and high carbon content, were chosen because they have the potential to be a low-cost and sustainable precursor for producing porous carbon. An inert atmosphere was created by purging the system with argon gas to ensure the carbonization process proceeded efficiently without oxidation. This inert environment was crucial for preventing combustion and ensuring the formation of high-quality porous carbon with well-developed porosity. In addition to the porous carbon, a synthetic wastewater solution containing 1% lead(II) chloride ($PbCl_2$) was prepared for the adsorption experiments. The $PbCl_2$ used in this study was $PbCl_2$ anhydrous, sourced from Sigma-Aldrich, with a reported purity of ≥ 98%. The use of this high-purity $PbCl_2$ enabled the adsorption process to be reliable and consistent by minimizing impurities. $PbCl_2$ salt was dissolved in demineralized water (DW) to avoid interference from ions or impurities present in tap water, leading to the formation of synthetic wastewater. This controlled environment allowed for a precise assessment of the porous carbon's adsorption efficiency, specifically for lead ions, thus providing accurate and reproducible data for the study.

Instrumentation

The carbonization process of the palm shell samples was carried out in a controlled environment

using an electric furnace under an inert argon atmosphere to prevent oxidation. A Linberg Blue M 1200 °C furnace from Thermo Fisher Scientific was used for this purpose, ensuring precise temperature control throughout the process. The samples were heated to 400, 600, and 800 °C to examine how carbonization temperature affects the characteristics of porous carbon. These temperatures were selected to optimize the carbonization process and identify the conditions that would result in the highest adsorption efficiency.

After carbonization, the resulting charcoal was ground into a uniform, fine powder using a disk mill, a crucial step to increase surface area and uniformity, which are key for maximizing adsorption. This powder was then analyzed using advanced techniques to examine its structural and chemical properties.

The PANalytical X'Pert Pro X-ray diffractometer (XRD) was used to analyze porous carbon samples and evaluate their crystallinity and phase composition. This method revealed how different carbonization temperatures affected the structural transformation, providing data on the degree of graphitization and the presence of crystalline regions. Additionally, Fourier transform infrared spectroscopy (FTIR) with the Agilent 5500 Series was performed to identify functional groups present on the surface of the porous carbon. FTIR analysis revealed specific chemical bonds and surface features that play a role in the adsorption process, particularly regarding lead ions.

A Jeol JSM-6510LA scanning electron microscope (SEM) was utilized to observe the porous carbon's surface morphology and pore structure. High-resolution SEM images provided insight into the size and distribution of pores in the material, which are crucial for understanding how well lead ions are absorbed. The SEM analysis highlighted the well-developed pore network necessary to effectively absorb contaminants from aqueous solutions.

Thermal properties of the palm kernel shell (PKS) were also analyzed to understand its thermal stability and behavior during carbonization. Differential scanning calorimetry (DSC) was used to examine the heat flow associated with thermal transitions, while thermal gravimetric analysis (TGA) tracked the weight loss of the samples as the temperature rose, providing important insights into the decomposition stages and thermal degradation of the material.

After adsorption, residual Pb^{2+} concentrations in solutions were measured by Thermo Scientific's iCAP 6000 series ICP-OES. This highly precise technique allowed for an accurate assessment of the porous carbon's performance under different carbonization conditions.

Procedure

Dehydration and carbonization process

The palm shell samples were first subjected to a dehydration step to ensure the removal of moisture and improve the efficiency of the carbonization process. This involved placing the raw palm shell samples in an oven set at 120 °C, where they were heated until they reached a constant weight, indicating the complete evaporation of moisture content. This step was critical in preparing the samples for carbonization, as any residual moisture could interfere with the formation of porous carbon and potentially disrupt the development of the material's porous structure.

After dehydration, the dried palm shell samples were transferred to an electric furnace for carbonization. The process was conducted under a continuous flow of argon gas to create an inert atmosphere. Argon, an inert gas, was essential for preventing oxidation of the samples at high temperatures. Oxygen exposure during carbonization could result in combustion or partial oxidation, which would have a negative impact on the quality and adsorption properties of the resulting porous carbon. By maintaining an oxygen-free environment, the carbonization process could proceed efficiently, ensuring that the samples underwent the necessary chemical transformations to become high-quality porous carbon, as illustrated in Fig. 1.

The carbonization temperature of 400, 600, and 800 °C was chosen to study how temperature affects the material's structural and adsorption properties. Each temperature was maintained for 1 h, ensuring sufficient time for the thermal degradation of non-carbon components, such as volatile organic compounds, while promoting the development of the carbon matrix. These

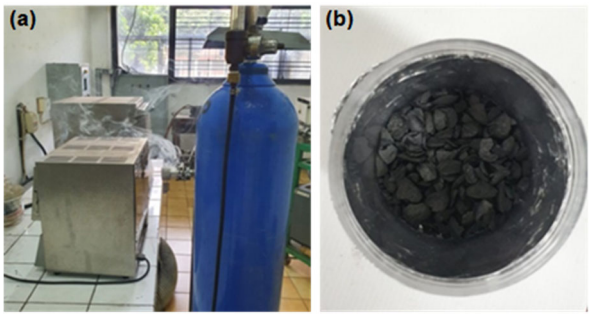

Fig 1. Carbonization process with (a) flowing argon gas; (b) PKS charcoal after carbonization process

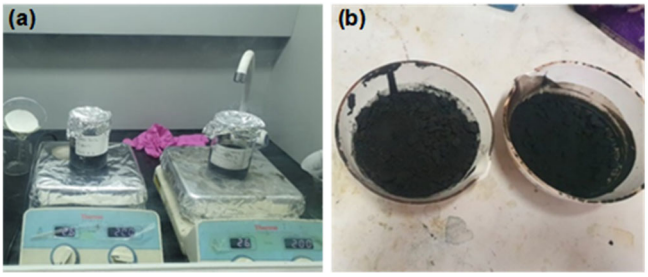

Fig 2. Activation process on sample: (a) process of stirring charcoal with activator solution, (b) activated charcoal

specific temperatures were chosen to explore a range of carbonization conditions, from lower temperatures that favor the preservation of functional groups to higher temperatures that enhance porosity and surface area by driving off more volatiles and restructuring the carbon. The 1 h duration at each temperature was optimized to balance the thermal decomposition of the material while preventing excessive loss of carbon content. All adsorption experiments were then performed at constant temperature to evaluate the Pb^{2+} adsorption capacity of the resulting materials.

Post-carbonization processing and adsorption testing

After carbonization, the produced charcoal was finely ground into a consistent powder using a disk mill. This process achieved a consistent particle size, essential for maximizing surface area and improving adsorption efficiency in subsequent tests. The powdered porous carbon was mixed with 100 mL of a synthetic wastewater solution containing 1% $PbCl_2$ to simulate lead contamination. The effectiveness of Pb^{2+} removal using porous carbon is influenced by both the adsorbent weight and the volume of the aqueous $PbCl_2$ solution, which play critical roles in achieving optimal adsorption. By using a controlled solution, the focus remained on evaluating the removal efficiency of Pb^{2+} ions without interference from other impurities.

The porous carbon was stirred with the solution in a glass beaker using a magnetic stirrer (Fig. 2(a)) with varying contact times set at 1, 2, and 3 h based on the carbonization temperature used. This thorough mixing promoted better interaction between the porous carbon and Pb^{2+}, allowing the adsorption process to proceed efficiently. After the stirring phase, the mixture was filtered to isolate the carbon particles, and the filtered porous carbon (Fig. 2(b)) underwent further analysis to assess its adsorption performance. These analyses involved measuring the remaining concentration of Pb^{2+} in the solution to evaluate the effectiveness of the porous carbon in reducing Pb^{2+} levels and to determine its capacity for Pb^{2+} uptake. This study specifically examines the effect of carbonization temperature on the adsorption efficiency of porous carbon derived from PKS. While factors such as the adsorbent's weight and solution volume can influence Pb^{2+} removal [14], they are kept constant and fall outside the scope of this research. The primary goal is to isolate the effects of carbonization conditions.

■ RESULTS AND DISCUSSION

Thermal Decomposition and Pore Formation in PKS Biomass

Figs. 3 and 4 present DSC-TGA graphs illustrating the heat flow and mass change of palm shell samples as a function of temperature. The data reveals a multi-step degradation process that begins with the breakdown of moisture, followed by hemicellulose, cellulose, and lignin, and ultimately results in the formation of a carbon-rich material. The loss of mass between 50 and 150 °C is the result of the physical water evaporation from the PKS matrix. This phase is primarily an endothermic process with no chemical decomposition, as indicated by the DSC curve (Fig. 3), resulting in a minor reduction in mass due to the release of moisture (Fig. 4). As the temperature rises above 150 °C, hemicellulose, the least

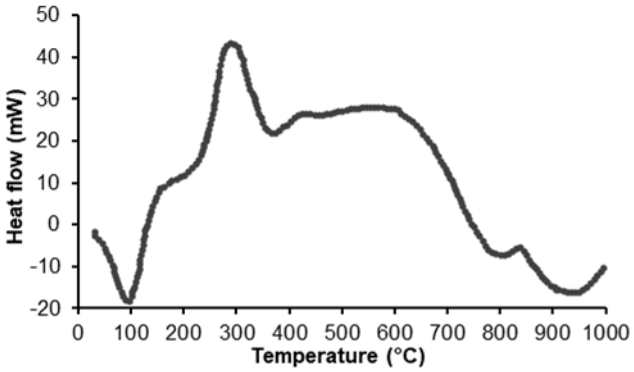

Fig 3. Graph of heat flow during heating of PKS

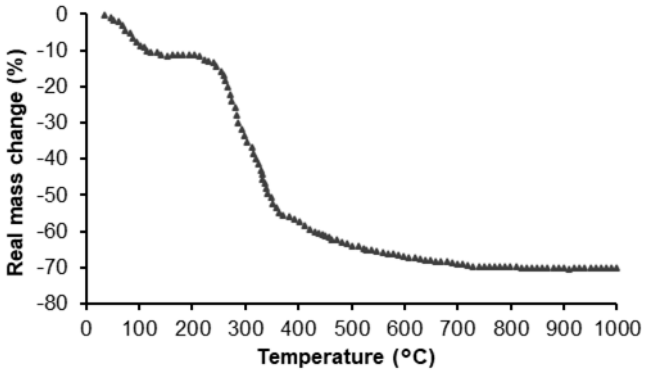

Fig 4. Graph of mass degradation during heating of PKS

thermally stable component, begins to decompose. The process continues until it reaches around 300 °C, which causes the release of volatile organic compounds like CO_2, CO, and light gases. The decomposition of hemicellulose is accompanied by significant mass loss. This is an exothermic reaction, suggesting that some energy stored in the organic components of the PKS is released during this phase [15].

After the hemicellulose degrades, cellulose decomposition follows, releasing energy and transforming the biomass into a porous structure [9]. Lignin, the most thermally stable component, starts breaking down between 300 and 800 °C. Unlike hemicellulose and cellulose, lignin decomposes slowly, resulting in gradual, sustained mass loss. Lignin's degradation produces char, volatile organic molecules, and gases, enhancing porosity through mesopore formation. The slow decomposition of lignin supports carbonization, which begins around 400 °C [16]. Once temperatures exceed 400 °C, carbonization becomes the primary reaction, driving off remaining volatile organic materials and converting the biomass into solid carbon. By 800 °C, approximately 70% of the initial biomass has been converted into gases and volatiles, leaving behind a carbon-rich char with a well-developed porous structure. Though mass loss continues, the rate slows as fewer volatile components remain. The carbonization process creates micropores and mesopores, significantly boosting the material's adsorption capacity [17].

The development of the pore structure is crucial for the effectiveness of the porous carbon produced [18]. The diffusion of larger molecules into the material is further enhanced by the presence of mesopores that emerge later during lignin decomposition and carbonization. As temperatures rise, the porous material becomes more porous and the pore size decreases, particularly after 500 °C, making it suitable for applications such as heavy metal absorption from wastewater [19]. A complex and multi-stage process is involved in the thermal decomposition of PKS, which transforms biomass into carbon-rich material with a highly porous structure. Both micropores and mesopores are developed during the carbonization process, which is driven by increasing temperature, to enhance the material's adsorption properties. This continuous evolution of the structure makes the final product ideal for environmental remediation applications, particularly for the adsorption of contaminants like heavy metals. The DSC-TGA data proves that the production of a material with exceptional adsorption potential is a result of the sequential breakdown of organic components, followed by carbonization [20].

Structural Analysis of Porous Carbon: Crystallinity and Porosity

The crystallinity of porous carbon derived from PKS was evaluated using both XRD and FTIR. The degree of crystallinity increased with higher carbonization temperatures, as reflected in the sharper peaks observed in the XRD patterns at 2θ angles of 22.37°, 22.78°, and 22.84° (Fig. 5). The presence of crystalline regions within the carbon matrix is indicated by these peaks, which became more evident at higher temperatures. The relative crystallinity of the samples rose

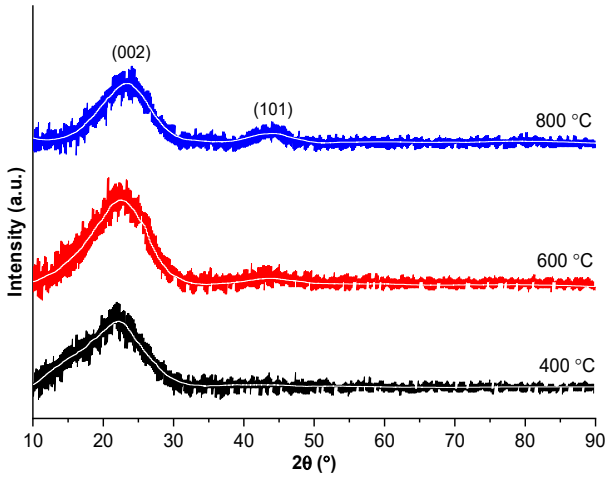

Fig 5. Graph of XRD results of PKS after carbonization

from 28.4% at 400 °C to 34.1% at 800 °C, which can be seen in Table 1. This rise in crystallinity is accompanied by a reduction in the distance between layers (from 3.97 Å at 400 °C to 3.89 Å at 800 °C), and a decrease in crystallite size from 12.4 to 11.9 Å, further confirming the structural reorganization that occurs at elevated temperatures.

Despite the rise in crystallinity, the porous carbon retains its amorphous nature, which contributes to its high porosity. This is an important feature for adsorption applications, as the amorphous regions provide extensive micropore and mesopore networks that enhance the material's adsorption properties. The findings are consistent with prior studies [21] that demonstrate the importance of maintaining an amorphous-carbon balance for optimal adsorption capacity.

A quantitative XRD analysis in Table 1 confirms that crystallinity increases with higher carbonization temperatures. For instance, the relative crystallinity at 400 °C was 28.4%, increasing to 31.5% at 600 °C, and further rising to 34.1% at 800 °C. This rise in crystallinity is attributed to the reorganization of the carbon structure, accompanied by an expansion in interplanar spacing and the development of additional pores. The peak at 22.84° (2θ) suggests that the structure becomes more ordered but remains predominantly amorphous due to incomplete crystallization. Despite the increase in crystallinity, the amorphous nature of the material is essential to maintain a high surface area for adsorption applications [22]. The trend in Table 1 illustrates that the distance between layers decreases slightly as the carbonization temperature increases, reflecting the ordering of the carbon structure. Although the crystalline regions do not significantly grow in size, the material retains a significant amorphous framework, which is crucial for adsorption processes. The amorphous regions help maintain a high surface area necessary for effective adsorption [21].

In addition to XRD analysis, FTIR was used to examine changes in functional groups caused by carbonization and activation processes (Fig. 6). Fig. 6 presents the absorption spectrum, revealing several key features. At a wavenumber of 3,708 cm^{-1}, the absorption band observed matches the O–H functional group [22]. This band shifts to 3,691 and 3,620 cm^{-1} due to vibrational changes in the functional group as the temperature increases. The methyl (CH_3) and methylene (CH_2) groups exhibit C–H stretching vibrations, detected

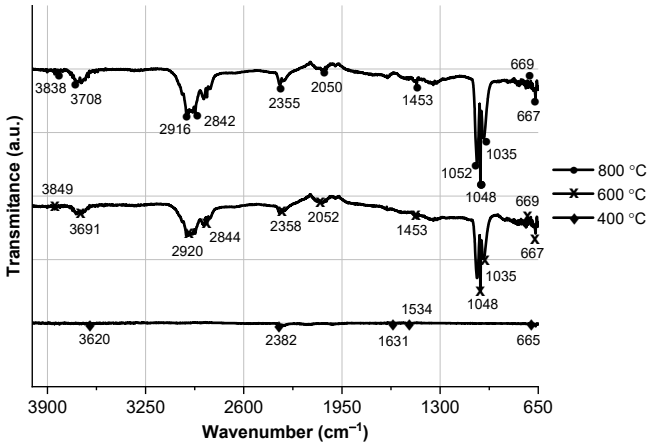

Fig 6. Graph of FTIR results of PKS after carbonization

Table 1. Table of XRD results of PKS after carbonization

Temperature (°C)	Crystallinity relative (%)	Peak (002) position (°)	Distance between layer (Å)	Crystallite size (Å)	Number of layer
400	28.4	22.37	3.97	12.4	3
600	31.5	22.78	3.90	11.8	3
800	34.1	22.84	3.89	11.9	3

in the range of 2,842–2,920 cm^{-1} [23]. At 400 °C, these peaks are prominent, indicating the presence of aliphatic groups. However, at 600 °C, their intensity decreases, suggesting the degradation of aliphatic chains. By 800 °C, these peaks disappear entirely, indicating the complete transformation into aromatic carbon structures [22].

Additional peaks at 2,382, 2,358, 2,355, 2,052, and 2,050 cm^{-1} are associated with carbon structures, including triplet patterns, while a peak at 1,453 cm^{-1} signifies C=C aromatic vibrations [24]. The intensity of the aromatic C=C peaks increases with temperature, confirming the formation of a more graphitic and stable carbon structure at higher carbonization temperatures. The range of 1,035–1,052 cm^{-1} reflects C–O bond vibrations [23]. The peak at 1,035 cm^{-1} is initially prominent at 400 °C but diminishes significantly at 800 °C, indicating a reduction in oxygen-containing functional groups. These changes illustrate the decreasing polarity and volatility of the material as it transitions into a more stable carbon framework.

The Morphological Structure of Activated PKS

The morphological features of the activated PKS were analyzed using SEM after subjecting the samples to different activation temperatures. As shown in Fig. 7, the SEM images revealed that increasing the activation temperature led to more defined and extensive pore formation on the surface. At 400 °C, the surface exhibited fewer and less pronounced pores. However, at 800 °C, the surface was significantly more porous, displaying an extensive network of micropores and mesopores. This progression indicates that higher activation temperatures facilitate the development of a more porous structure, which is crucial for adsorption applications. The reduction in particle size with increasing temperature was also evident, with particle sizes decreasing from 173 µm at 400 °C to 34 µm at 800 °C. This reduction enhances the material's surface area, further contributing to its adsorption capabilities by by providing shorter diffusion pathways for Pb^{2+} to reach the interior pores of the carbon matrix [25]. The decomposition of volatile components during the carbonization process was responsible for creating these channels and cavities within the carbon matrix, which form the basis for the micropores and mesopores.

Following the carbonization process, the produced charcoal underwent further treatment to optimize its adsorption performance. The charcoal was finely ground into a consistent powder using a disk mill, reducing particle size and increasing surface area. This post-carbonization grinding step ensured better exposure of the pores formed during the carbonization process. The porous carbon was then used in adsorption testing with synthetic wastewater to assess its effectiveness in reducing Pb^{2+} levels. During the adsorption process, the interaction between the porous carbon and the Pb^{2+} was facilitated by thorough mixing, which promoted the utilization of the existing pores [26]. While the intrinsic porous structure was primarily established during the carbonization and activation processes, the post-carbonization treatments played a crucial role in optimizing the accessibility and utilization of these pores, thereby enhancing the adsorption efficiency of the material.

The formation of pores at higher temperatures is caused by the decomposition of volatile compounds in

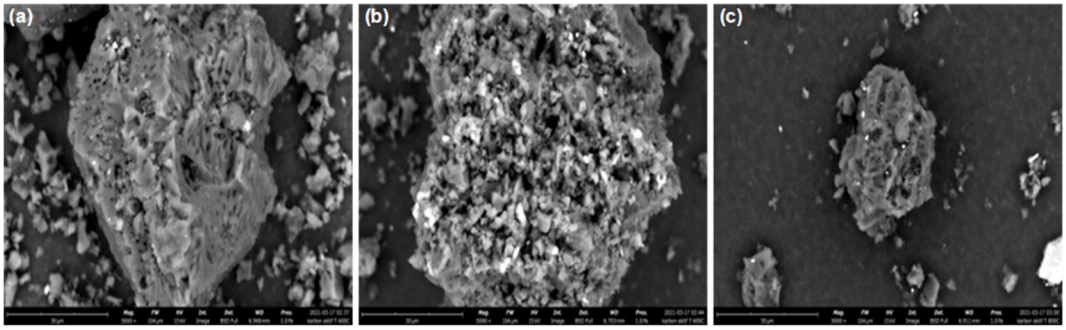

Fig 7. Microstructural SEM images of the activated PKS at (a) 400, (b) 600, (c) 800 ℃ activated temperature

the raw material, which results in the formation of channels and cavities in the carbon structure [27]. The formation of these smaller pores is particularly beneficial as they provide the porous carbon with a larger surface area, enhancing its capacity to adsorb contaminants. The breakdown of lignocellulosic components in the palm kernel shells, facilitated by high temperatures, results in a carbon-rich framework, increasing the material's effectiveness for adsorption purposes [28].

The Adsorption Capacity of Porous Carbon

The adsorption capacity of porous carbon was significantly influenced by both the carbonization temperature and the duration of contact with the contaminant. The efficacy of porous carbon extracted from palm kernel shells in removing Pb^{2+} from an aqueous $PbCl_2$ solution was evaluated. As shown in Fig. 8, the maximum adsorption efficiency was achieved at a carbonization temperature of 800 °C with a contact duration of 3 h, significantly reducing $PbCl_2$ concentration from 10,000 to 7,250 ppm. This corresponds to an adsorption capacity of around 27.5%. Conversely, the lowest efficiency was observed at 400 °C with a contact time of 1 h. This condition led to a minimal decrease in $PbCl_2$ concentration, reducing it from 10,000 to 9,880 ppm. The adsorption efficiency under these conditions was just 1.2% [29].

The superior performance at higher temperatures is attributed to the increase in pore volume and the reduction in pore size, enhancing the material's ability to trap and adsorb lead ions [17]. This observation aligns with the formation of micropores and mesopores during carbonization, significantly boosting the surface area available for adsorption. Additionally, as the carbonization temperature rises, more well-defined pores develop, improving the diffusion and uptake of larger molecules [15] like lead ions.

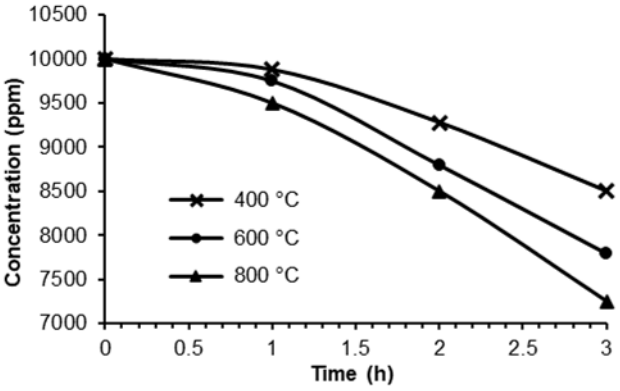

Fig 8. Decrease in $PbCl_2$ concentration over time during the adsorption capacity test of activated PKS at different temperatures

Longer contact times also contributed to higher adsorption efficiency, allowing more time for the interaction between the Pb^{2+} and the porous carbon surface [29]. This finding aligns with previous studies showing that extended exposure times enhance the binding of adsorbates to the adsorbent, further boosting adsorption capacity. Determining the optimal contact time is crucial, as it maximizes the efficiency of the adsorption process [30].

Although the adsorption capacity of the porous carbon in this study was lower than that reported in some previous studies, which achieved over 90% Pb^{2+} removal efficiency under varying conditions [5]. The findings offer valuable insights into how carbonization temperature, pore structure, and adsorption efficiency are interrelated. As highlighted by this study, the adsorption capabilities of porous carbon for environmental remediation purposes [6] can be enhanced by optimizing carbonization temperature and contact time.

Adsorption Kinetics and Mechanistic Modeling for Lead Ion Removal

Fig. 9 illustrates the relationship between equilibrium concentration (C_e) in solution and adsorption capacity (q_e) of porous carbon derived from PKS for the Pb^{2+} adsorption. The adsorption equilibrium was modeled using the Freundlich isotherm equation (Eq. (1)) [31]

$$\ln q_e = \ln K_F + \frac{1}{n}\ln C_e \quad (1)$$

The experimental data were fitted using the Freundlich isotherm model, a commonly applied framework for describing adsorption processes on heterogeneous surfaces. The slope (1/n) of 1 suggests that $n < 1$, suggesting that the adsorption mechanism is predominantly chemisorption [32].

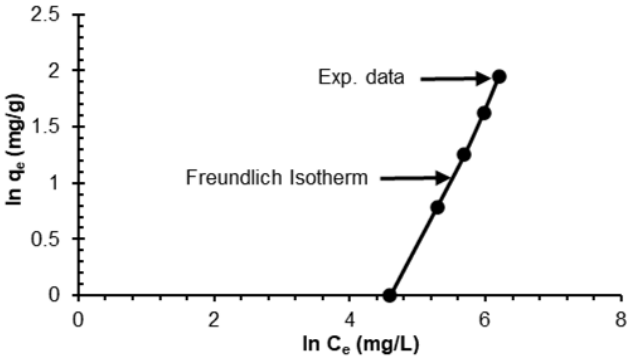

Fig 9. Freundlich equilibrium isotherms for the system Pb^{2+}-porous carbon

A modeling plot of ln C_e versus ln q_e produced a Freundlich constant (n) of 0.8327 and K_F of 0.003916, reflecting the material's adsorption capacity. Notably, the coefficient of determination ($R^2 = 0.9981$) indicates an excellent fit of the Freundlich isotherm model to the experimental data. This strong correlation underscores the model's suitability for describing the adsorption behavior of Pb^{2+} ions on the porous carbon material, affirming its heterogeneous adsorption characteristics [33].

The graph reveals that the q_e increases with higher C_e, indicating that the porous carbon retains significant adsorption sites even at elevated Pb^{2+} concentrations. This behavior demonstrates the material's potential for practical applications in treating solutions with high lead ion concentrations. However, the low K_F value highlights the need for further optimization to enhance the material's adsorption capacity.

The adsorption kinetics in 1 h contact time of Pb^{2+} onto porous carbon derived from PKS were systematically analyzed across three different carbonization temperatures: 400, 600, and 800 °C. These temperatures were selected to investigate the influence of thermal activation on the structural and chemical properties of the carbon material and their subsequent effects on adsorption performance. The adsorption kinetic was modeled using pseudo-first-order (PFO) and pseudo-second-order (PSO) equations as illustrated in Fig. 10 to evaluate the mechanism of adsorption and the nature of interactions between Pb^{2+} and the adsorbent surface. The results clearly indicate that both adsorption capacity and kinetics are influenced by carbonization temperature, with optimal performance observed at 800 °C. However, the experimental data show that the PFO model does not accurately represent the adsorption kinetics at any of the three temperatures. This is evident from the relatively low R^2 value compared with that of PSO and notable differences between the predicted and experimental q_e, as detailed in Table 2.

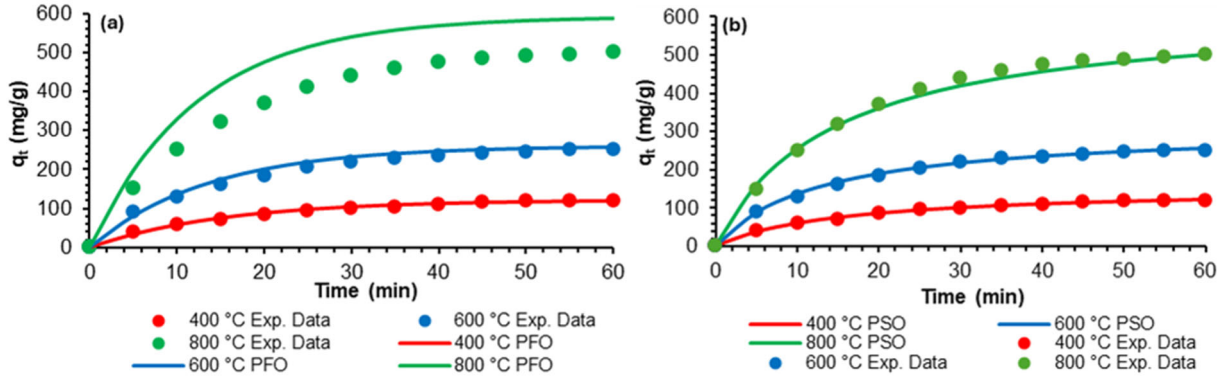

Fig 10. (a) Pseudo first order and (b) pseudo second order reaction kinetics for system Pb^{2+} - porous carbon

Table 2. Table of result parameters of pseudo-first-order and pseudo-second-order models

T (°C)	Pseudo-first-order			Pseudo-second-order		
	q_e (mg/g)	k_1 (1/min)	R^2	q_e (mg/g)	k_2 (1/min)	R^2
400	122.3395	0.0645	0.9821	153.8462	0.00041	0.9965
600	261.1774	0.0739	0.9921	312.5000	0.00025	0.9984
800	591.0496	0.0812	0.9905	625.0000	0.00011	0.9965

The PFO model, which assumes a physical adsorption mechanism and attributes the process to a rate-limiting diffusion step [34], fails to capture the complexity of the adsorption behavior observed in this study. Notably, at 800 °C, the q_e values predicted by the PFO model are significantly lower than the experimental results, underscoring the model's inability to account for the influence of chemical interactions and enhanced porosity on the adsorption process. Although the PFO rate constant (k_1) slightly increases with rising temperatures, this trend does not adequately explain the substantial improvements in adsorption capacity and kinetics observed experimentally.

In contrast, the PSO model demonstrates an excellent fit to the experimental data, with R^2 values exceeding 0.996 at all temperatures. This strong correlation indicates that the adsorption process is primarily governed by chemisorption, involving valence forces through the sharing or exchange of electrons between Pb^{2+} ions and functional groups on the carbon surface [35]. The equilibrium adsorption capacities predicted by the PSO model align closely with the experimental values, confirming its suitability for describing the kinetic behavior. Moreover, the PSO rate constant (k_2) increases substantially with rising carbonization temperatures, highlighting the enhanced reactivity of the adsorbent surface. This improvement can be attributed to increased porosity, larger surface area, and the activation of oxygen-containing functional groups such as carboxyl, hydroxyl, and lactone [36].

The temperature-dependent trends observed in this study underscore the critical role of thermal activation in determining the physicochemical properties of the carbon material. Higher carbonization temperatures lead to increased surface area, enhanced and the formation of active functional groups, all of which contribute to improved adsorption performance. The presence of oxygen-containing functional groups on the carbon surface enhances the affinity of the adsorbent for Pb^{2+} ions, enabling the formation of stable complexes that result in high adsorption capacities [37].

■ CONCLUSION

This study demonstrates the high effectiveness of porous carbon derived from PKS in adsorbing Pb^{2+} from aqueous solutions. The porous carbon produced at a carbonization temperature of 800 °C showed the highest efficiency, reducing Pb^{2+} concentrations by 27.5%. These results emphasize the importance of optimizing carbonization conditions to enhance the performance of porous carbon for adsorption applications. The Freundlich isotherm model best describes the adsorption behavior, indicating multilayer adsorption on a heterogeneous surface. This suggests that the porous carbon effectively adsorbs Pb^{2+} at various sites. Kinetic analysis supports this, showing alignment with the PSO model, highlighting physical mechanisms as the main drivers. The rapid adsorption, enabled by the material's large surface area and well-developed porosity, confirms its suitability for water purification and environmental remediation. Overall, this study demonstrates that palm kernel shell-derived porous carbon is a viable, sustainable, and economical solution for reducing Pb^{2+} contamination, making it a promising option for eco-friendly water treatment applications.

■ ACKNOWLEDGMENTS

We acknowledge the invaluable guidance offered by The Institute for Research and Community Service (LPPM) at the Republic of Indonesia Defense University (RIDU) and the Program Study of Materials Science at Universitas Indonesia (UI). We also express our gratitude to the Indonesia National Research and Innovation Agency (BRIN) for providing research facilities.

■ CONFLICT OF INTEREST

The authors declare do not have any conflict of interest.

■ AUTHOR CONTRIBUTIONS

Mas Ayu Elita Hafizah conducted data curation, formal analysis, investigation, methodology, and writing the original draft. Azwar Manaf conducted conceptualization, formal analysis, supervision, validation, writing review, and editing. Tiara Valency conducted data curation, investigation, and methodology. Andreas conducted methodology, software, validation and visualization. Maykel Manawan

conducted formal analysis, methodology, resources, software, and validation. All authors agreed to the final version of this manuscript.

■ REFERENCES

[1] Husin, S., Wijaya, C., Ghafur, A.H.S., Machmud, T.M.Z., and Mardanugraha, E., 2023, Palm oil downstream strategy: Enhancing Indonesia's bargaining position in international palm oil trade, *Migr. Lett.*, 20 (5), 678–689.

[2] Li, T.M., 2018, After the land grab: Infrastructural violence and the "Mafia System" in Indonesia's oil palm plantation zones, *Geoforum*, 96, 328–337.

[3] Januari, A.D., and Agustina, H., 2022, Palm oil empty fruit bunches and the implementation of zero waste and renewable energy technologies, *IOP Conf. Ser.: Earth Environ. Sci.*, 1034, 012004.

[4] Sridhar, M.K.C., and AdeOluwa, O.O., 2009, "Palm Oil Industry Residues" in *Biotechnology for Agro-Industrial Residues Utilisation: Utilisation of Agro-Residues*, Eds. Singh nee' Nigam, P., and Pandey, A., Springer, Dordrecht, Netherlands, 341–55.

[5] Faisal, M., Gani, A., and Fuadi, Z., 2021, Utilization of activated carbon from palm kernel shells as the bioadsorbent of lead waste, *Int. J. GEOMATE*, 20 (78), 81–86.

[6] Resdiansyah, R., Mohd Ujang, A., and Zaini, Z., 2017, Bio-asphalt concrete: From waste product to green aggregate replacement, *Pertanika J. Sci. Technol.*, 25, 145–154.

[7] Akintunde, M.A., 2012, The effects of paper and palm kernel shell on mechanical properties of sawdust briquettes, *IOSR J. Mech. Civ. Eng.*, 4 (4), 11–16.

[8] Olele, P.C., Nkwocha, A.C., Ekeke, I.C., and Ileagu, M.O., and Okeke, E.O., 2016, Assessment of palm kernel shell as friction material for brake pad production, *Int. J. Eng. Manage. Res.*, 6 (1), 281–284.

[9] Wu, H., Dong, Z., Sun, J., and Ding, K., 2024, Boosting the adsorption capacity of activated carbon prepared from *Amygdalus communis* shells using physicochemical co-activation method, *Biomass Convers. Biorefin.*, 14 (15), 18121–18131.

[10] Lawtae, P., and Tangsathitkulchai, C., 2021, The use of high surface area mesoporous-activated carbon from longan seed biomass for increasing capacity and kinetics of methylene blue adsorption from aqueous solution, *Molecules*, 26 (21), 6521.

[11] Hoang, A.T., Kumar, S., Lichtfouse, E., Cheng, C.K., Varma, R.S., Senthilkumar, N., Phong Nguyen, P.Q., and Nguyen, X.P., 2022, Remediation of heavy metal polluted waters using activated carbon from lignocellulosic biomass: An update of recent trends, *Chemosphere*, 302, 134825.

[12] Balali-Mood, M., Naseri, K., Tahergorabi, Z., Khazdair, M.R., and Sadeghi, M., 2021, Toxic mechanisms of five heavy metals: Mercury, lead, chromium, cadmium, and arsenic, *Front. Pharmacol.*, 12, 643972.

[13] Hama Aziz, K.H., Mustafa, F.S., Omer, K.M., Hama, S., Hamarawf, R.F., and Rahman, K.O., 2023, Heavy metal pollution in the aquatic environment: efficient and low-cost removal approaches to eliminate their toxicity: A review, *RSC Adv.*, 13 (26), 17595–17610.

[14] Liu, S., Cui, S., Guo, H., Wang, Y., and Zheng, Y., 2021, Adsorption of lead ion from wastewater using non-crystal hydrated calcium silicate gel, *Materials*, 14 (4), 842.

[15] Rashidi, N.A., and Yusup, S., 2019, Production of palm kernel shell-based activated carbon by direct physical activation for carbon dioxide adsorption, *Environ. Sci. Pollut. Res.*, 26, 33732–33746.

[16] Phothong, K., Tangsathitkulchai, C., and Lawtae, P., 2021, The analysis of pore development and formation of surface functional groups in bamboo-based activated carbon during CO_2 activation, *Molecules*, 26 (18), 5641.

[17] Andas, J., Rahman, M.L.A., and Yahya, M.S.M., 2017, Preparation and characterization of activated carbon from palm kernel shell, *IOP Conf. Ser.: Mater. Sci. Eng.*, 226 (1), 012156.

[18] Harper, G., Sommerville, R., Kendrick, E., Driscoll, L., Slater, P., Stolkin, R., Walton, A., Christensen, P., Heidrich, O., Lambert, S., Abbott, A., Ryder, K., Gaines, L., and Anderson, P., 2019, Recycling

lithium-ion batteries from electric vehicles, *Nature*, 575 (7781), 75–86.

[19] Díez, D., Urueña, A., Piñero, R., Barrio, A., and Tamminen, T., 2020, Determination of hemicellulose, cellulose, and lignin content in different types of biomasses by thermogravimetric analysis and pseudocomponent kinetic model (TGA-PKM method), *Processes*, 8 (9), 1048.

[20] Sorek, N., Yeats, T.H., Szemenyei, H., Youngs, H., and Somerville, C.R., 2014, The implications of lignocellulosic biomass chemical composition for the production of advanced biofuels, *BioScience*, 64 (3), 192–201.

[21] Destyorini, F., Irmawati, Y., Hardiansyah, A., Widodo, H., Yahya, I.N.D., Indayaningsih, N., Yudianti, R., Hsu, Y.I., and Uyama, H., 2021, Formation of nanostructured graphitic carbon from coconut waste via low-temperature catalytic graphitization, *Eng. Sci. Technol., Int. J.*, 24 (2), 514–523.

[22] Hadjiivanov, K.I., Panayotov, D.A., Mihaylov, M.Y., Ivanova, E.Z., Chakarova, K.K., Andonova, S.M., and Drenchev, N.L., 2021, Power of infrared and Raman spectroscopies to characterize metal-organic frameworks and investigate their interaction with guest molecules, *Chem. Rev.*, 121 (3), 1286–1424.

[23] Dostert, K.H., O'Brien, C.P., Mirabella, F., Ivars-Barceló, F., and Schauermann, S., 2016, Adsorption of acrolein, propanal, and allyl alcohol on Pd(111): A combined infrared reflection–absorption spectroscopy and temperature programmed desorption study, *Phys. Chem. Chem. Phys.*, 18 (20), 13960–13973.

[24] Nandiyanto, A.B.D., Ragadhita, R., and Fiandini, M., 2022, Interpretation of Fourier transform infrared spectra (FTIR): A practical approach in the polymer/plastic thermal decomposition, *Indones. J. Sci. Technol.*, 8, 113–126.

[25] Spencer, W., Ibana, D., Singh, P., and Nikoloski, A.N., 2024, Effect of surface area, particle size and acid washing on the quality of activated carbon derived from lower rank coal by KOH activation, *Sustainability*, 16 (14), 5876.

[26] Chen, W., Chen, Y., Wang, Y., and Zhao, N., 2024, Combining activated carbon adsorption and CO_2 carbonation to treat fly ash washing wastewater and recover high-purity calcium carbonate, *Water*, 16 (20), 2896.

[27] Hidayu, A.R., and Muda, N., 2016, Preparation and characterization of impregnated activated carbon from palm kernel shell and coconut shell for CO_2 capture, *Procedia Eng.*, 148, 106–113.

[28] Hisbullah, H., Kana, S., Nabila, N., and Faisal, M., 2022, Characterization of physically and chemically activated carbon derived from palm kernel shells, *Int. J. GEOMATE*, 23 (97), 203–210.

[29] Mouni, L., Merabet, D., Bouzaza, A., and Belkhiri, L., 2011, Adsorption of Pb(II) from aqueous solutions using activated carbon developed from Apricot stone, *Desalination*, 276 (1), 148–153.

[30] Boonsombuti, A., Phinichkha, N., Supansomboon, S., and Luengnaruemitchai, A., 2023, The use of lignin from palm kernel shell (PKS) to fabricate oil palm mesocarp fiber (OPMF) particleboards, *Int. J. Adhes. Adhes.*, 125, 103425.

[31] Al-Harby, N.F., Albahly, E.F., and Mohamed, N.A., 2021, Kinetics, isotherm and thermodynamic studies for efficient adsorption of Congo red dye from aqueous solution onto novel cyanoguanidine-modified chitosan adsorbent, *Polymers*, 13 (24), 4446.

[32] Budhiary, K.N.S., and Sumantri, I., 2021, Langmuir and Freundlich isotherm adsorption using activated charcoal from banana peel to reduce total suspended solid (TSS) levels in tofu industry liquid waste, *IOP Conf. Ser.: Mater. Sci. Eng.*, 1053 (1), 012113.

[33] Kaushal, A., and Singh, S.K., 2017, Critical analysis of adsorption data statistically, *Appl. Water Sci.*, 7 (6), 3191–3196.

[34] Abd Wahab Sha'arani, S., Ros Saidon Khudri, M.A.M., Othman, A.R., Halmi, M.I.E., Yasid, N.A., and Shukor, M.Y., 2019, Kinetic analysis of the adsorption of the brominated flame retardant 4-bromodiphenyl ether onto biochar-immobilized

Sphingomonas sp., *Biorem. Sci. Technol. Res.*, 7 (1), 8–12.

[35] Anjum, A., Mazari, S.A., Hashmi, Z., Jatoi, A.S., Abro, R., Bhutto, A.W., Mubarak, N.M., Dehghani, M.H., Karri, R.R., Mahvi, A.H., and Nasseri, S., 2023, A review of novel green adsorbents as a sustainable alternative for the remediation of chromium (VI) from water environments, *Heliyon*, 9 (5), e15575.

[36] Tran, H.N., 2023, Applying linear forms of pseudo-second-order kinetic model for feasibly identifying errors in the initial periods of time-dependent adsorption datasets, *Water*, 15 (6), 1231.

[37] Xie, N., Wang, H., and You, C., 2024, Enhanced adsorption of Pb^{2+} by the oxygen-containing functional groups enriched activated carbon, *Environ. Sci. Pollut. Res.*, 31 (21), 31028–31041.